FULL PAPER

Dalton
www.rsc.org/dalton

A novel 2D arsenic vanadate network grafted with a transition metal complex: $[Cu(phen)]_2[V^{IV}V_4{}^{V}As_2O_{19}]\cdot 0.5H_2O$ †

Yangguang Li,[a] Gejihu De,[a] Mei Yuan,[a] Enbo Wang,*[a,b] Rudan Huang,[a] Changwen Hu,[a] Ninghai Hu[c] and Hengqing Jia[c]

[a] *Institute of Polyoxometalate Chemistry, Department of Chemistry, Northeast Normal University, Changchun, 130024, P. R. China. E-mail: wangenbo@public.cc.jl.cn*

[b] *State Key Laboratory of Structural Chemistry, Fujian Institute of Research on the Structure of Matter, Chinese Academy of Sciences, Fuzhou, 350002, P. R. China*

[c] *Changchun Institute of Applied Chemistry, Chinese Academy of Sciences, Changchun, 130022, P. R. China*

Received 28th October 2002, Accepted 10th December 2002
First published as an Advance Article on the web 10th January 2003

A novel organic–inorganic hybrid compound $[Cu(phen)]_2[V^{IV}V_4{}^{V}As_2{}^{V}O_{19}]\cdot 0.5H_2O$ **1** has been hydrothermally synthesized. Its structure, determined by single crystal X-ray diffraction, exhibits an unusual two-dimensional arsenic vanadate layered network grafted with the $[Cu(phen)]^{2+}$ complex. The chelating phen ligands project perpendicularly beyond the inorganic layer. Variable temperature magnetic susceptibility studies indicate that both ferro- and antiferro-magnetic interactions exist in **1**.

Introduction

A current focus in polyoxovanadate chemistry is the rational design and preparation of novel organic–inorganic hybrid oxovanadium clusters in order to explore their potential applications in catalysis, electron conductivity, magnetism and photochemistry.[1–4] In this field, an important recent advance is the modification of inorganic vanadium oxides with various organic ligands and transition metal complexes or fragments. The introduction of transition metal-ligand units can not only enrich the frameworks of vanadium oxides but also ameliorate their electronic and magnetic properties.[5–8] Based on this strategy, numerous organic–inorganic hybrid phases belonging to the $\{M_xL_y/V/O\}$ and $\{M_xL_y/V/P/O\}$ systems (M = transition metal, L = organic ligand) have been isolated, which exhibit interesting one- (1D), two- (2D) and three-dimensional (3D) frameworks.[9–19] Compared with abundant compounds in the {V/P/O} system, however, limited studies have been made on the {V/As/O} system. In the past few years, reports have been concentrated on the discrete arsenic vanadate clusters[20–24] exemplified by $K_6[As_6V_{15}O_{42}(H_2O)]\cdot 8H_2O$[20] and anionic porous skeletons such as $MVOAsO_4$ (M = Na, Li, NH_4)[23] and $[Cs_3(VO)_2(V_2O_3)(AsO_4)(HAsO_4)_2]$.[24] Recently, the introduction of a hydrothermal technique and the use of organic templating agents has led to the production of some arsenic vanadate phases with 2D layer-like and 3D porous structures, such as $[H_2NC_4H_8NH_2][(VO)_2(HAsO_4)_2(H_2AsO_4)_2]$[25] and $[AsV^{IV}{}_8V^{V}{}_2O_{26}(H_2O)]\cdot 8H_2O$,[26] in which the organic templates act as counter cations or structural filling agents. However, the inorganic {V/As/O} substructures decorated with or linked by transition metal-ligand complexes have not been reported yet. Since vanadium–oxide–phosphate systems exhibit extensive coordination chemistry with the transition metal complexes, the solids constructed from the {V/As/O} system may also have potential for the incorporation of appropriate metal-ligand moieties. This offers the opportunity for preparing new organic–inorganic hybrid materials containing inorganic {V/As/O} scaffolds decorated with transition metal-ligand functional units.

In this paper, we report a novel organic–inorganic hybrid arsenic vanadate, $[Cu(phen)]_2[V^{IV}V_4{}^{V}As_2{}^{V}O_{19}]\cdot 0.5H_2O$ (phen = *o*-phenanthroline) **1**, which contains an unusual 2D {V/As/O} network with the $[Cu(phen)]^{2+}$ fragments coordinated directly to the inorganic layer. To our knowledge, **1** represents the first example of an inorganic arsenic vanadate backbone grafted with the transition metal complex. The variable temperature magnetic susceptibility of **1** has also been studied.

Experimental

Physical measurements

Elemental analyses (C, H and N) were performed on a Perkin-Elmer 2400 CHN Elemental Analyzer. As, Cu and V were determined by a Leaman inductively coupled plasma (ICP) spectrometer. The IR spectrum of **1** was recorded in the range 400–4000 cm^{-1} on an Alpha Centaurt FT/IR spectrophotometer using a KBr pellet. EPR spectra were recorded on a Japanese JES–FE3AX spectrometer at 293 K. TG analysis was performed on a Perkin-Elmer TGA7 instrument in flowing N_2 with a heating rate of 10 °C min^{-1}. Variable temperature magnetic susceptibility was measured (SQUID, Quantum Design) in the temperature range of 2–300 K at 5000 Oe.

Synthesis

All chemicals purchased were of reagent grade and used without further purification. Compound **1** was hydrothermally synthesized under autogenous pressure. The starting materials $CuCl_2\cdot 2H_2O$ (0.5 mmol), NH_4VO_3 (0.5 mmol), $Na_2HAsO_4\cdot 7H_2O$ (0.5 mmol), As_2O_5 (0.125 mmol) and phen (1.0 mmol) were dissolved in 9 mL H_2O in the mole ratio 4 : 4 : 4 : 1 : 8 : 4000 and stirred for 2 h. The solution was sealed in a 20 mL Teflon-lined reactor and heated at 180 °C for 72 h. Then the autoclave was cooled at 10 °C h^{-1} to room temperature. The resulting black block crystals **1** were filtered off, washed with water, and dried at ambient temperature (yield 60% based on vanadium). Elemental analysis; found: C, 23.7; H, 1.5; N, 4.6; As, 12.3; Cu, 10.4; V, 20.9; Calc. for $C_{24}H_{17}As_2Cu_2N_4O_{19.5}V_5$: C, 23.9; H, 1.4; N, 4.7; As, 12.4; Cu, 10.5; V, 21.1%. IR spectrum (cm^{-1}): 3423(s, br), 1617(m), 1513(m), 1425(s), 1425(s), 1143(m), 1003(s), 980(s), 849(s), 784(s), 722(m), 669(s), 680(w), 649(m), 616(m), 490(s).

† Electronic supplementary information (ESI) available: packing diagram, IR spectrum, TG curve and a plot of χ_M *versus* T for **1**. See http://www.rsc.org/suppdata/dt/b2/b210589f/

DOI: 10.1039/b210589f

Crystallography

Crystal data for **1** were collected on a Rigaku R-AXIS RAPID IP diffractometer using graphite monochromated Mo-Kα radiation (λ = 0.71073 Å) at 293 K. Data processing was accomplished with the SAINT processing program. Empirical absorption correction (ψ scans) was applied. The structure was solved by the direct method and refined by full-matrix least-squares on F^2 using the SHELXTL crystallographic software package.[27] All the non-hydrogen atoms were refined anisotropically. The hydrogen atoms were located from difference Fourier maps. Structure solution and refinement based on 3885 independent reflections with $I > 2\sigma(I)$ and 266 parameters gave $R_1(wR_2) = 0.0268\ (0.0866)$ $\{R_1 = \Sigma||F_o| - |F_c||/\Sigma|F_o|;\ wR_2 = \Sigma[w(F_o^2 - F_c^2)^2]/\Sigma[w(F_o^2)^2]^{1/2}\}$. A summary of the crystal data and structure refinement for compound **1** is provided in Table 1. The selected bond lengths and angles are listed in Table 2.

CCDC reference number 188034.

See http://www.rsc.org/suppdata/dt/b2/b210589f/ for crystallographic data in CIF or other electronic format.

Table 1 Crystal data and structure refinement of **1**

Empirical formula	$C_{24}H_{17}As_2Cu_2N_4O_{19.5}V_5$
Formula weight	1205.04
Temperature/K	293(2)
Crystal system	Monoclinic
Space group	$P2_1/c$
a/Å	11.4154(10)
b/Å	10.0380(5)
c/Å	14.8841(9)
β/°	93.411(4)
Volume/Å^3, Z	1702.5(2), 2
Absorption coefficient/mm^{-1}	4.558
F(000)	1168
Crystal size/mm	0.571 × 0.209 × 0.185
Reflections collected	6673
Independent reflections	3885 (R_{int} = 0.0176)
Absorption correction	Empirical
Refinement method	Full-matrix least-squares on F^2
Data/restraints/parameters	3885/0/266
Final R indices[$I > 2\sigma(I)$]	$R1$ = 0.0268, $wR2$ = 0.0866
R indices (all data)	$R1$ = 0.0356, $wR2$ = 0.0950

Table 2 Bond lengths (Å) and angles (°) of **1**

Cu–O(1)	1.930(2)	Cu–N(1)	2.003(3)
Cu–O(3)#1	1.916(2)	Cu–N(2)	2.012(3)
V(1)–O(5)	1.890(2)	V(1)–O(7)	1.590(5)
V(1)–O(5)#2	1.942(2)	V(1)–O(4)	1.987(2)
V(1)–O(4)#2	2.016(2)	V(2)–O(8)	1.592(3)
V(2)–O(5)	1.914(2)	V(2)–O(6)	1.965(2)
V(2)–O(4)	2.003(2)	V(2)–O(9)#3	1.688(3)
V(3)–O(10)	1.599(3)	V(3)–O(9)	1.888(3)
V(3)–O(5)	1.919(2)	V(3)–O(6)	1.997(2)
V(3)–O(2)#2	1.967(2)	As–O(2)	1.671(2)
As–O(3)	1.655(2)	As–O(4)	1.728(2)
As–O(1)	1.672(2)		
O(1)–Cu–N(1)	171.56(10)	O(1)–Cu–N(2)	90.95(11)
N(1)–Cu–N(2)	82.17(12)	O(1)–Cu–O(3)#1	96.35(9)
O(7)–V(1)–O(4)	109.3(2)	O(7)–V(1)–O(5)	111.0(2)
O(7)–V(1)–O(4)#2	108.1(2)	O(5)–V(1)–O(4)	77.56(10)
O(7)–V(1)–O(5)#2	108.3(2)	O(8)–V(2)–O(9)#3	109.9(2)
O(8)–V(2)–O(6)	102.80(13)	O(8)–V(2)–O(5)	114.03(16)
O(8)–V(2)–O(4)	100.59(13)	O(5)–V(2)–O(6)	76.00(9)
O(6)–V(2)–O(4)	149.41(10)	O(5)–V(2)–O(4)	76.61(9)
O(10)–V(3)–O(9)	107.50(17)	O(10)–V(3)–O(5)	107.54(14)
O(9)–V(3)–O(5)	144.93(15)	O(10)–V(3)–O(6)	106.04(13)
O(9)–V(3)–O(6)	93.85(10)	O(5)–V(3)–O(6)	75.12(9)
O(3)–As–O(2)	113.83(11)	O(3)–As–O(1)	111.55(11)
O(1)–As–O(4)	107.15(11)	O(3)–As–O(4)	105.37(11)
OW ⋯ O(2)	3.283	OW ⋯ O(7)	2.301

#1 $-x, -y + 1, -z$; #2 $-x, -y, -z$; #3 $-x, y + 1/2, -z + 1/2$.

Results and discussion

Crystal structure of compound 1

The single crystal structure analysis suggests that complex **1** consists of a novel arsenic vanadate layer coordinated with $[Cu(phen)]^{2+}$. The crystal water molecules occupy the interlayer space. In the basic unit of compound **1** (see Fig. 1), the

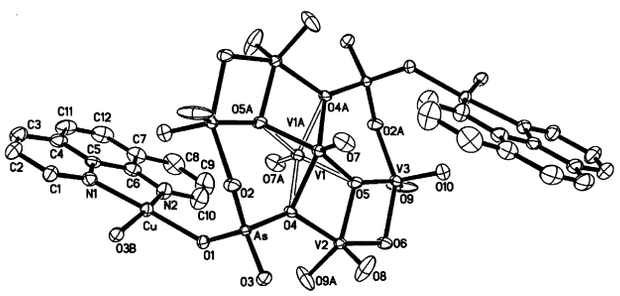

Fig. 1 ORTEP[30] drawing of compound **1** with thermal ellipsoids at 50% probability. H atoms and water molecules are omitted for clarity.

Cu(II) centers exhibit $\{CuN_2O_2\}$ quadrilateral geometry coordinated with two nitrogen donors of phen groups and two oxygen atoms of two adjacent $\{AsO_4\}$ tetrahedral units. The average Cu–N and Cu–O bond lengths are 2.008 and 1.923 Å, respectively. The O–Cu–N angles vary from 90.95(11) to 171.56(10)° (Table 2). Two As centers possess a distorted $\{AsO_4\}$ tetrahedral environment. The As–O distances are in the range of 1.655(2)~1.728(2) Å and O–As–O angles 105.37(11)~113.83(11)°. All vanadium centers have a distorted $\{VO_5\}$ square pyramidal environment. Each V atom bonds to a terminal oxygen atom and four bridging oxygen atoms with V–O distances in the range of 1.590(5)~1.997(2) Å and O–V–O angles 80.0°~157.5°. It is noteworthy that the V(1)–O(7) group is disordered and occupies two opposite sites (as shown in Fig. 1), each site possessing a 50% occupancy.

An unusual structural feature is that **1** exhibits a novel {As/V/O} inorganic layer based on the fundamental building unit $\{V_5As_2O_{19}\}$ as shown in Fig. 2. In the $\{V_5As_2O_{19}\}$ unit, all

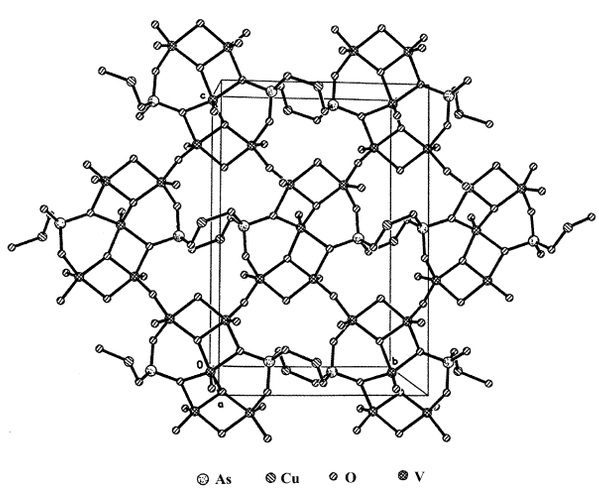

Fig. 2 View of the 2D Cu–As–V oxide skeleton on the *bc* plane.

the $\{VO_5\}$ square pyramids connect with each other by edge-sharing oxygen atoms and form an interesting Z-type pentavanadate as shown in Fig. 3. The two $\{AsO_4\}$ tetrahedral units are linked with the Z-type vanadate through two corner oxygen atoms O(2) and O(4). Therefore, a three-membered ring (3-MR) $\{AsV_2O_3\}$ is formed from the $\{V(1)O_5\}$, $\{V(3)O_5\}$ and $\{AsO_4\}$ units *via* a corner-sharing mode. Furthermore, the adjacent $\{V_5As_2O_{19}\}$ units are linked together *via* V(2)–O(9)–

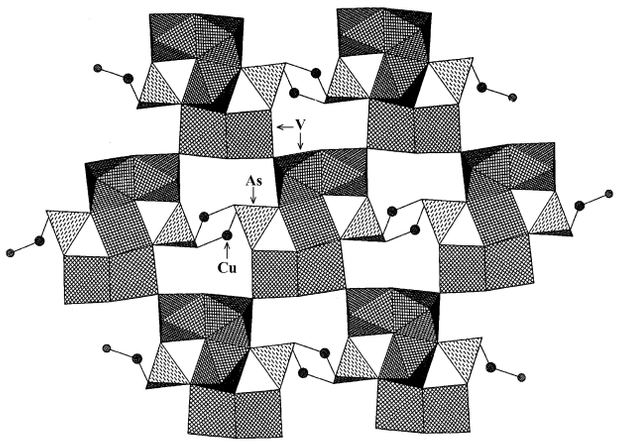

Fig. 3 Polyhedral representation of the 2D Cu–As–V oxide layer.

V(3) bridges to form a 2-D layered framework with a large ten-membered ring (10-MR) $\{As_2V_8O_{12}\}$. The most interesting structural feature of **1** is that two $[Cu(phen)]^{2+}$ coordination complexes are grafted onto the arsenic vanadate layer. These complex cations act as bridges linking with adjacent $\{V_5As_2O_{19}\}$ units *via* two oxygen atoms on the $\{AsO_4\}$ units. Two Cu centers and two $\{AsO_4\}$ units exhibit a 4-MR $\{Cu_2As_2O_4\}$. It is also noteworthy that the 4-MR $\{Cu_2As_2O_4\}$ moieties are vertical to the layer of vanadium arsenic oxide. To our knowledge, such an inorganic arsenic vanadate backbone grafted with the transition metal complex has not been observed before.

In the packing arrangement, the π–π stacking interactions between interlayer phen groups play an important role in stabilization of the structure of **1**. The chelating phen ligands project perpendicularly beyond the wave-like layer. Adjacent phen groups in **1** are parallel to each other and separated on average by *ca.* 3.33 Å. Therefore, the 2D layers of **1** are further extended into a 3D supramolecular array. The dissociated water molecules occupy the interlayer space and connect with oxygen atoms of the inorganic layer *via* strong hydrogen bonding interactions (as shown in Table 2).

Charge balance considerations and the black coloration of crystalline **1** indicate that there exist mixed-valent vanadium sites in this compound. The bond valence sum calculations[28] give values of 4.2, 5.0 and 4.7 for V(1), V(2) and V(3), indicating that the V(1) site is in the +4 oxidation state, while the other vanadium sites are in the +5 oxidation state. Furthermore, the calculation values of 1.92 and 5.07 for Cu and As show the existence of Cu^{2+} and As^{5+}. This result is also proved by EPR spectra (as shown in Fig. 4). The EPR spectrum of **1** at room temperature shows a V^{4+} signal with $g = 2.09$ and a Cu^{2+} signal with $g = 2.06$, in accordance with the valence sum calculations.

IR Spectrum and thermal analysis of 1

In the IR spectrum of **1** (Fig. S2, ESI), the bands at 849, 784, 722 and 669 cm^{-1} are due to the ν(V=O) or ν(V–O–V) vibrations. While the strong peak at 1003 cm^{-1} is attributed to the vibrations of As–O bands. Bands in the 1617–1143 cm^{-1} region are attributed to characteristic peaks of phen groups. The broad band at 3423 cm^{-1} is characteristic of H_2O molecules.

The TG curve of compound **1** (Fig. S3, ESI) is divided into three stages. The first weight loss is 0.6% in the temperature range 120–150 °C, corresponding to the loss of water molecules. The second weight loss is 4.6% in the temperature range 320–360 °C. The third weight loss is 26.1% from 400 to 510 °C. These two continuous weight losses are ascribed to the release of phen groups. The whole weight loss (31.3%) is in agreement with the calculated value (30.7%). The sample does not lose weight at temperatures higher than 510 °C.

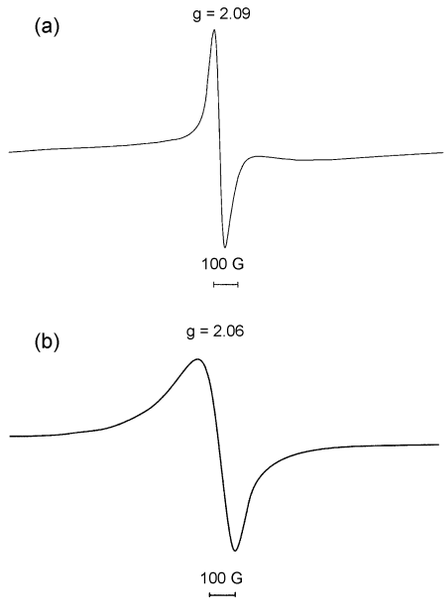

Fig. 4 The EPR spectra of **1**: (a) V^{4+} and (b) Cu^{2+}.

Magnetic properties of 1

The variable temperature magnetic susceptibility was measured from 2 to 300 K at 5000 Oe for **1**. The thermal variations of $\chi_M T$ and $1/\chi_M$ are displayed in Fig. 5. The plot of $\chi_M T$ *versus* T shows a value of 0.72 emu K Oe^{-1} mol^{-1} at 150 K, and continuously increases on cooling to a value of 0.94 emu K Oe^{-1} mol^{-1} at 10 K. From 10 to 5 K, the curve rises abruptly to a value of 1.19 emu K Oe^{-1} mol^{-1}. This behavior for the $\chi_M T$ curve shows that a ferromagnetic interaction exists in **1**. However, the curve drops abruptly below 4 K, indicating that an antiferromagnetic interaction exists in **1** at lower temperature. The inverse susceptibility plot as a function of temperature is linear above 4 K, following the Curie–Weiss law with $C = 0.73$ emu K Oe^{-1} mol^{-1} and $\theta = 3.025$ K. According to this result, it could be presumed that the unpaired electrons in the Cu^{2+} ($3d^9$) and V^{4+} ($3d^1$) centers might have the same spin direction above 4 K (T_N), resulting in ferromagnetic interactions, while the antiferromagnetic interactions below T_N might be due to the cancellation of spin. The field dependence

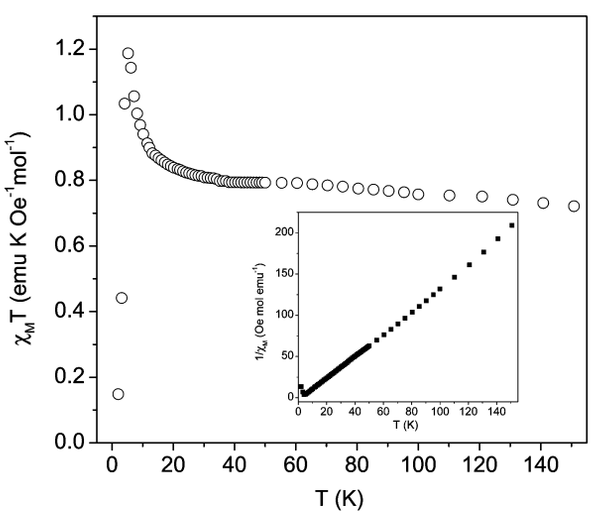

Fig. 5 Plot of $\chi_M T$ *vs.* temperature for **1**; the inset shows the inverse susceptibility with a linear regression based upon the Curie–Weiss law.

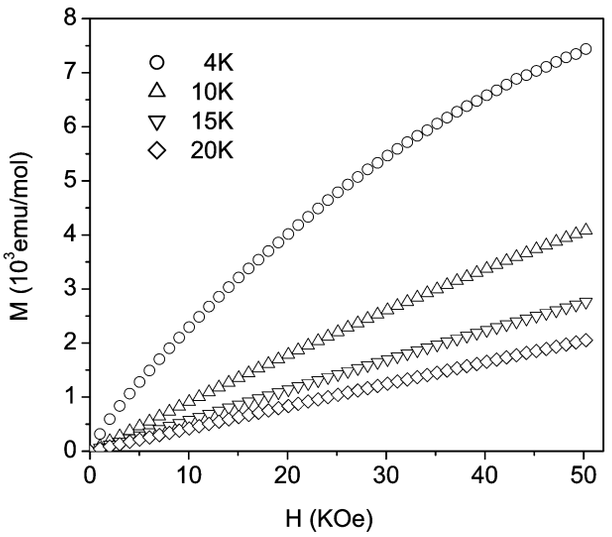

Fig. 6 Field dependence of magnetization at 4, 10, 15 and 20 K for **1**.

of magnetization was measured at 4, 10, 15 and 20 K (Fig. 6). At 15 and 20 K, the $M(H)$ behavior is paramagnetic. At 4 K (less prominent at 10 K), the $M(H)$ slope decrease at high field is characteristic of metamagnetism.[29] This again confirms that both ferromagnetic and antiferromagnetic interactions occur in compound **1**.

In summary, the successful synthesis of $[Cu(phen)]_2[V^{IV}V_4^{V}As_2^{V}O_{19}]\cdot 0.5H_2O$ provides a model for the preparation of novel materials belonging to the $\{M_xL_y/V/As/O\}$ system (M = transition metal, L = organic ligand). Extended research on the structural chemistry of this system may focus on the replacement of copper and phen with other transition metals and organic ligands. Studies in this respect are underway to reveal the synthetic rules and to explore their attractive properties.

Acknowledgements

This work was financially supported by the National Natural Science Foundation of China (20171010).

References

1 (*a*) L. C. W. Baker and D. C. Glick, *Chem. Rev.*, 1998, **98**, 3; (*b*) P. Gouzerh and A. Proust, *Chem. Rev.*, 1998, **98**, 77.
2 D. W. Murphy and P. A. Christian, *Science*, 1979, **205**, 651.
3 P. J. Hagrman, D. Hagrman and J. Zubieta, *Angew. Chem., Int. Ed.*, 1999, **38**, 2638.
4 T. Chirayil, P. Y. Zavalij and M. S. Whittingham, *Chem. Mater.*, 1998, **10**, 2629.
5 P. J. Hagrman and J. Zubieta, *Inorg. Chem.*, 2000, **39**, 3252.
6 P. J. Hagrman, R. C. Finn and J. Zubieta, *Solid State Sci.*, 2001, **3**, 745.
7 Y. P. Zhang, J. R. D. DeBord, C. J. O'Connor, R. C. Haushalter, A. Clearfield and J. Zubieta, *Angew. Chem., Int. Ed. Engl.*, 1996, **35**, 989.
8 R. L. LaDuca, Jr., R. S. Rarig, Jr. and J. Zubieta, *Inorg. Chem.*, 2001, **40**, 607.
9 Y. G. Li, E. B. Wang, H. Zhang, G. Y. Luan, C. W. Hu, N. H. Hu and H. Q Jia, *J. Solid State Chem.*, 2002, **163**, 10.
10 Y. Lu, E. B. Wang, M. Yuan, G. Y. Luan and Y. G. Li, *J. Chem. Soc., Dalton Trans.*, 2002, 3029.
11 M. Yuan, Y. G. Li, E. B. Wang, Y. Lu, C. W. Hu, N. H. Hu and H. Q. Jia, *J. Chem. Soc., Dalton Trans.*, 2002, 2916.
12 W. S. You, E. B. Wang, Y. Xu, Y. G. Li L Xu and C. W. Hu, *Inorg. Chem.*, 2001, **40**, 5468.
13 (*a*) Z. Shi, S. H. Feng, L. R. Zhang, G. Y. Yang and J. Hua, *Chem. Mater.*, 2000, **12**, 2930; (*b*) Z. Shi, S. H. Feng, S. Gao, L. R. Zhang, G. Y. Yang and J. Hua, *Angew. Chem., Int. Ed.*, 2000, **39**, 2325.
14 X.-M. Zhang, M.-L. Tong, S.-H Feng and X.-M. Chen, *J. Chem. Soc., Dalton Trans.*, 2001, 2069.
15 X. M. Zhang, M. L. Tong and X. M Chen, *Chem. Commun.*, 2000, 1817.
16 C. M. Liu, Y. L. Hou, J. Zhang and S. Gao, *Inorg. Chem.*, 2002, **41**, 140.
17 C. H. Huang, L. H. Huang and K. H. Lii, *Inorg. Chem.*, 2001, **40**, 2625.
18 L. H. Huang, H. M. Kao and K. H. Lii, *Inorg. Chem.*, 2002, **41**, 2936.
19 L. M. Zheng, X. Q. Wang, Y. S. Wang and A. J. Jacobson, *J. Mater. Chem.*, 2001, **11**, 1100.
20 A. Müller and J. Döring, *Angew. Chem., Int. Ed. Engl.*, 1988, **27**, 1721.
21 A. Müller, M. Pewk and J. Döring, *Inorg. Chem.*, 1991, **30**, 4935.
22 M. I. Khan, Q. Chew and J. Zubieta, *Inorg. Chim. Acta*, 1992, **91**, 97.
23 (*a*) A. Haddad, T. Jouini and Y. Piffard, *Eur. J. Solid State Inorg. Chem.*, 1992, **29**, 57; (*b*) R. C. Haushalter, Q. Chen, V. Songhornonian, J. Zubieta and C. J. O'Connor, *J. Solid State Chem.*, 1994, **108**, 128; (*c*) J. Ganbicher, F. Orsini, T. Le Mercier, S. Llorente, A. Villesuzanne and M. Quarton, *J. Solid State Chem.*, 2000, **150**, 250.
24 S. L. Wang and Y. H. Lee, *Inorg. Chem.*, 1994, **33**, 3845.
25 R. C. Haushalter, E. Wang, L. M. Meyer, S. S. Dhengra, M. E. Thompson and J. Zubieta, *Chem. Mater.*, 1994, **9**, 1463.
26 (*a*) W. M. Bu, L. Ye, G. Y. Yang, M. C. Shao, Y. G. Fan and J. Q. Xu, *Chem. Commun.*, 2000, 1279; (*b*) Y. N. Zhao, Q. S. Liu, Y. F. Li, X. M. Chen and Z. H. Mai, *J. Mater. Chem.*, 2001, **11**, 1553.
27 (*a*) G. M. Sheldrick, SHELXS 97, Program for Crystal Structure Solution, University of Göttingen, 1997; (*b*) G. M. Sheldrick, SHELXL 97, Program for Crystal Structure Refinement, University of Göttingen, 1997.
28 D. Brown and D. Altermatt, *Acta Crystallogr., Sect. B*, 1985, **41**, 244.
29 R. K. Chiang, C. C. Huang and C. S. Wur, *Inorg. Chem.*, 2001, **40**, 3237.
30 M. N. Burnett and C. K. Johnson, ORTEP-III: Oak Ridge Thermal Ellipsoid Plot Program for Crystal Structure Illustrations, Report ORNL-6895, Oak Ridge National Laboratory, Oak Ridge, TN, USA, 1996.